

# Molecular Imaging and Biology

## Assessing human embryonic stem cell-derived dopaminergic neuron progenitor transplants using non-invasive imaging techniques

--Manuscript Draft--

<b>Manuscript Number:</b>	MIBI-D-20-00017R1	
<b>Full Title:</b>	Assessing human embryonic stem cell-derived dopaminergic neuron progenitor transplants using non-invasive imaging techniques	
<b>Article Type:</b>	Original Article	
<b>Funding Information:</b>	UK Regenerative Medicine Platform (MR/K026739/1)	Professor Patricia Murray
<b>Abstract:</b>	<p><b>Purpose:</b> Human pluripotent stem cell (hPSC)-derived dopaminergic neuron progenitor cells (DAPCs) are a potential therapy for Parkinson's disease (PD). However, their intracranial administration raises safety concerns including uncontrolled proliferation, migration and inflammation. Here, we apply a bimodal imaging approach to investigate the fate of DAPC transplants in the rat striatum.</p> <p><b>Procedures:</b> DAPCs co-expressing luciferase and ZsGreen or labelled with micron-sized particles of iron oxide (MPIOs) were transplanted in the striatum of RNU rats ( n = 6 per group). DAPCs were tracked in vivo using bioluminescence and magnetic resonance (MR) imaging modalities.</p> <p><b>Results:</b> Transgene silencing in differentiating DAPCs accompanied with signal attenuation due to animal growth rendered the bioluminescence undetectable by week two post-intrastratial transplantation. However, MR imaging of MPIO-labelled DAPCs showed that transplanted cells remained at the site of injection for over 120 days. Post-mortem histological analysis of DAPC transplants demonstrated that labelling with either luciferase/ZsGreen or MPIOs did not affect the ability of cells to differentiate into mature dopaminergic neurons. Importantly, labelled cells did not elicit increased glial reactivity compared to non-labelled cells.</p> <p><b>Conclusions:</b> In summary, our findings support the transplantation of hPSC-derived DAPCs as a safe treatment for PD.</p>	
<b>Corresponding Author:</b>	Christopher James Hill, PhD University of Liverpool Liverpool, UNITED KINGDOM	
<b>Corresponding Author Secondary Information:</b>		
<b>Corresponding Author's Institution:</b>	University of Liverpool	
<b>Corresponding Author's Secondary Institution:</b>		
<b>First Author:</b>	Masoumeh Mousavinejad	
<b>First Author Secondary Information:</b>		
<b>Order of Authors:</b>	Masoumeh Mousavinejad	
	Sophie Skidmore	
	Francesco Giovanni Barone	
	Pamela Tyers	
	Venkat Pisupati	
	Harish Poptani	
	Antonius Plagge	
	Roger Alistair Barker	
	Patricia Murray	
	Arthur Taylor	

	Christopher James Hill, PhD
<b>Order of Authors Secondary Information:</b>	
<b>Author Comments:</b>	Following review, one reviewer commented on the poor quality of main text figures in the pdf version of the manuscript. All figures have been submitted at high resolution, but the pdf conversion is significantly reducing this. Please can you advise on a way to show high resolution figures to the reviewer. I can supply high resolution figures in a compressed file if this would be helpful.
<b>Suggested Reviewers:</b>	<p>Laura Mezzanotte, PhD Associate Professor, Erasmus MC l.mezzanotte@erasmusmc.nl Dr Mezzanotte is an expert in the design of genetic reporters for multimodal in vivo cell tracking. She has extensive experience in the longitudinal imaging of cell grafts using bioluminescence. Further, she has explored the effects of lentiviral transduction and nanoparticle labelling on the phenotype of stem cell-derived progeny.</p> <p>Mathias Hoehn, PhD Professor, Max Planck Institute for Metabolome Research Mathias@sf.mpg.de Professor Hoehn is a world leader in intracranial stem cell tracking using MRI and optical imaging techniques. He has vast experience in the use of non-invasive imaging techniques to monitor the fate of transplanted stem cell grafts in the brain. Further, professor Hoehn's interests encompass the differentiation capacity of transplanted stem cells and their effects on host inflammatory response.</p> <p>Clare Parish, PhD Associate Professor, The University of Melbourne clare.parish@florey.edu.au Dr Parish's research is focused on the use of stem cell therapies to repair the injured brain. She has a particular focus on the use of pluripotent stem cell-derived dopaminergic neurons for the treatment of Parkinson's disease, and has explored the molecular basis of graft integration in the rodent brain.</p>



[Click here to view linked References](#)

1  
2  
3 **Assessing human embryonic stem cell-derived dopaminergic neuron**  
4 **progenitor transplants using non-invasive imaging techniques**  
5  
6  
7

8 Short title: Multimodal imaging of neural progenitor transplants  
9

10  
11  
12  
13 **M. Mousavinejad<sup>1</sup>, S. Skidmore<sup>1,3</sup>, F.G. Barone<sup>1</sup>, P. Tyers<sup>2</sup>, V. Pisupati<sup>3</sup>, H. Poptani<sup>1</sup>, A.**  
14 **Plagge<sup>1</sup>, R.A. Barker<sup>2,3</sup>, P. Murray<sup>1</sup>, A. Taylor<sup>1,5</sup> C.J. Hill<sup>1,4,5</sup>**  
15  
16  
17  
18  
19  
20

21 **Author information**  
22

23 <sup>1</sup>Department of Cellular and Molecular Physiology, Institute of Translational Medicine,  
24 University of Liverpool, Liverpool L69 3BX, UK  
25

26  
27  
28 <sup>2</sup>John van Geest Centre for Brain Repair & Department of Neurology, Department of Clinical  
29 Neurosciences, University of Cambridge, Cambridge, UK  
30

31  
32  
33 <sup>3</sup>WT-MRC Cambridge Stem Cell Institute, University of Cambridge, Cambridge, UK  
34

35  
36 <sup>4</sup>Centre for Women's Health Research, Department of Women's and Children's Health,  
37 Institute of Translational Medicine, University of Liverpool, Liverpool L8 7SS, UK  
38

39  
40 <sup>5</sup>Joint corresponding authors  
41  
42  
43  
44

45 To whom correspondence should be addressed:

46  
47 Dr Arthur Taylor

48  
49  
50 Email: [taylora@liverpool.ac.uk](mailto:taylora@liverpool.ac.uk)  
51

52  
53 Telephone: 0151 795 4456  
54

55 Dr Christopher Hill

56  
57 Email: [C.J.Hill1@liverpool.ac.uk](mailto:C.J.Hill1@liverpool.ac.uk)  
58

59  
60 Telephone: 0151 795 9584  
61  
62  
63  
64  
65

## Abstract

1  
2  
3 *Purpose:* Human pluripotent stem cell (hPSC)-derived dopaminergic neuron progenitor cells  
4  
5 (DAPCs) are a potential therapy for Parkinson's disease (PD). However, their intracranial  
6  
7 administration raises safety concerns including uncontrolled proliferation, migration and  
8  
9 inflammation. Here, we apply a bimodal imaging approach to investigate the fate of DAPC  
10  
11 transplants in the rat striatum.  
12  
13

14  
15 *Procedures:* DAPCs co-expressing luciferase and ZsGreen or labelled with micron-sized  
16  
17 particles of iron oxide (MPIOs) were transplanted in the striatum of RNU rats ( $n = 6$  per group).  
18  
19 DAPCs were tracked *in vivo* using bioluminescence and magnetic resonance (MR) imaging  
20  
21 modalities.  
22  
23

24  
25 *Results:* Transgene silencing in differentiating DAPCs accompanied with signal attenuation  
26  
27 due to animal growth rendered the bioluminescence undetectable by week two post-intrastratial  
28  
29 transplantation. However, MR imaging of MPIO-labelled DAPCs showed that transplanted  
30  
31 cells remained at the site of injection for over 120 days. Post-mortem histological analysis of  
32  
33 DAPC transplants demonstrated that labelling with either luciferase/ZsGreen or MPIOs did not  
34  
35 affect the ability of cells to differentiate into mature dopaminergic neurons. Importantly,  
36  
37 labelled cells did not elicit increased glial reactivity compared to non-labelled cells.  
38  
39  
40

41  
42 *Conclusions:* In summary, our findings support the transplantation of hPSC-derived DAPCs as  
43  
44 a safe treatment for PD.  
45  
46  
47  
48  
49  
50  
51  
52  
53  
54  
55  
56  
57  
58  
59  
60  
61  
62  
63  
64  
65

## Introduction

1  
2  
3  
4 Parkinson's disease (PD) is a neurodegenerative disease that results in part from the progressive  
5  
6 loss of dopaminergic (DA) neurons in the substantia nigra. Several groups have shown that  
7  
8 human pluripotent stem cell (hPSC)-derived dopaminergic neuron progenitor cells (DAPCs)  
9  
10 can generate mature DA neurons and improve motor function following intrastriatal  
11  
12 transplantation in animal models of PD [1-2]. This has now evolved to the point that first in  
13  
14 human hPSC-based DA neural transplants are being undertaken or planned in patients with PD.  
15  
16 However, prior to undertaking larger-scale clinical studies, animal experiments are needed to  
17  
18 adequately assess the safety of the therapies. Key safety concerns with such therapies for PD  
19  
20 and other central nervous system (CNS) disorders includes the risk that the implanted cells  
21  
22 could proliferate and form space occupying masses and/or migrate to off-target sites within the  
23  
24 CNS, and/or induce major neuroinflammation [3]. In addition to considering the potential risks,  
25  
26 it is also important to monitor the long-term viability and differentiation capacity of implanted  
27  
28 cells, as to be effective they must differentiate into the appropriate phenotype and persist in the  
29  
30 brain.  
31  
32  
33  
34  
35  
36  
37  
38

39 An effective strategy for monitoring the proliferation, viability and localisation of  
40  
41 implanted cells longitudinally is to employ a non-invasive imaging approach comprising  
42  
43 different modalities, such as bioluminescence (BLI), magnetic resonance (MRI) and  
44  
45 fluorescence imaging [4-5]. BLI is the most sensitive live animal imaging technique, enabling  
46  
47 relatively small numbers of transplanted cells to be detected [6]. This technique requires that  
48  
49 the cells express a luciferase reporter, which means that a signal is only emitted if the cells are  
50  
51 alive. An increase in BLI signal over time indicates cell proliferation and potential tumour  
52  
53 formation, whereas a loss of signal suggests that the cells are no longer viable. A drawback  
54  
55 with BLI, however, is that spatial resolution is poor, which means that it cannot be used to  
56  
57  
58  
59  
60  
61  
62  
63  
64  
65

1 determine the location of the implanted cells and/or any resultant masses within the brain. MR  
2 imaging, on the other hand, has a very high spatial resolution, and can accurately map the  
3 position of intracranial lesions [7]. Moreover, by labelling cells prior to administration with an  
4 appropriate contrast agent, such as iron oxide particles [8] or <sup>19</sup>F-based tracking agents [9],  
5 MRI can be used to plot the biodistribution of the cells over time.  
6  
7  
8  
9  
10

11  
12  
13         Hoehn and co-workers have shown previously that BLI and MR imaging can be used  
14 to monitor the viability and intracranial biodistribution of human embryonic stem cell (hESC)-  
15 derived neural stem cells following implantation into the mouse striatum [10]. To the best of  
16 our knowledge, this bimodal approach has not previously been used to track the  
17 tumourigenicity, viability and biodistribution of hESC-derived DAPCs, following intrastriatal  
18 administration into the rat brain. A key aim of this study, therefore, was to assess the potential  
19 of this bimodal BLI/MR strategy to track hESC-derived DAPCs *in vivo*. In addition to  
20 evaluating the effectiveness of the imaging modalities themselves, we also investigated  
21 whether the labels used for tracking (i.e. a Firefly luciferase, FLuc-ZsGreen bicistronic vector  
22 for BLI and iron oxide particles for MR imaging [4, 11]) affected the differentiation potential  
23 of the cells and/or their immunogenicity following implantation into the rat striatum.  
24  
25  
26  
27  
28  
29  
30  
31  
32  
33  
34  
35  
36  
37  
38  
39  
40  
41  
42  
43

## 44 **Materials and Methods**

### 45 **hESC culture and maintenance**

46  
47  
48  
49  
50  
51  
52  
53  
54  
55  
56  
57  
58  
59  
60  
61  
62  
63  
64  
65  
Clinical grade RC17 human embryonic stem cells (hESC) line were obtained from Roslin Cells Ltd., UK. Cells were expanded on laminin 521 (0.5 µg/cm<sup>2</sup>) (Biolamina) in iPS-Brew XF (StemMACS™). Cells were passaged as small clumps using Versene, a non-enzymatic cell dissociation reagent (ThermoFisher Scientific) and 10 µM of Rho kinase (Rock) inhibitor Y-

1  
2  
3  
4  
5  
6  
7  
8  
9  
10  
11  
12  
13  
14  
15  
16  
17  
18  
19  
20  
21  
22  
23  
24  
25  
26  
27  
28  
29  
30  
31  
32  
33  
34  
35  
36  
37  
38  
39  
40  
41  
42  
43  
44  
45  
46  
47  
48  
49  
50  
51  
52  
53  
54  
55  
56  
57  
58  
59  
60  
61  
62  
63  
64  
65

27632 dihydrochloride (StemMACS, Miltenyi) was added to the medium for the first 24 h after plating. Medium was changed daily and cells were maintained at 37°C under 5% CO<sub>2</sub>.

### **Generation of hESC reporter line and labelling with iron oxide particles**

RC17 cells were transduced with a lentiviral vector encoding for the bicistronic expression of the codon optimised firefly luciferase (luc2) and ZsGreen (via an IRES link) under the constitutive promoter, elongation factor- $\alpha$  (EF1 $\alpha$ ). The vector plasmid was a gift from Bryan Welm (Addgene plasmid #39196) and the production and titration of viral particles was carried out using established protocols [11]. In order to transduce the hESCs, colonies of undifferentiated RC17 cells were dissociated into very small clumps consisting of about 10-15 cells using Versene for 5 min. After centrifugation, the cells were counted and seeded onto laminin 521 at a density of approximately  $2.5 \times 10^4$  cells/cm<sup>2</sup> in the presence of 10  $\mu$ M Y-27632. Cells were incubated overnight and transduced on the following day with  $25 \times 10^4$  viral particles (multiplicity of infection of approximately 5) in the presence of polybrene (10  $\mu$ g/mL). After 24 h, the medium was replaced and the cells were expanded for 4 days prior to sorting for ZsGreen expression with a BD FACSAria (BD Biosciences) flow sorter. The Fluc-ZsGreen<sup>+</sup> cells were collected in iPS-Brew culture medium supplemented with 10  $\mu$ M Y-27632, seeded on laminin 521 and expanded for subsequent experiments. To assess bioluminescence activity, cells were plated at different densities in black 96-well plates (Thermo Scientific), allowed to settle for 2-4 h and then incubated with medium containing D-luciferin (150  $\mu$ g/mL, Promega) prior to data acquisition with an IVIS spectrum system (Perkin Elmer).

Micron-sized particles of iron oxide (MPIO) were used as a label for MR detection of DAPCs. Suncoast Yellow MPIOs (Bangs Beads, 1.63  $\mu$ m nominal diameter, Bangs Laboratories, Inc) were added directly to the DAPC's cell culture medium at a concentration of 1500 particles per

1  
2  
3  
4  
5  
6  
7  
8  
9  
10  
11  
12  
13  
14  
15  
16  
17  
18  
19  
20  
21  
22  
23  
24  
25  
26  
27  
28  
29  
30  
31  
32  
33  
34  
35  
36  
37  
38  
39  
40  
41  
42  
43  
44  
45  
46  
47  
48  
49  
50  
51  
52  
53  
54  
55  
56  
57  
58  
59  
60  
61  
62  
63  
64  
65

$\mu\text{L}$  for 24 h. After the labelling period, cells were carefully washed with PBS to remove unbound particles, harvested and then used for *in vivo* studies. The extent of MPIO labelling was assessed with a FACSCalibur (BD Biosciences) flow cytometer.

### **Differentiation into neural precursors and mature neurons**

RC17 cells were differentiated toward mesencephalic dopaminergic progenitor cells (DAPC) or terminally differentiated into mature dopaminergic (DA) neurons as previously described [12]. In brief, DAPCs are obtained after neuralisation, patterning and expansion of the cells for a period of 16 days, whereas DA neurons are obtained via the maturation of DAPCs for 34 days. Correct caudalization of progenitors towards a midbrain fate was achieved using 0.9  $\mu\text{M}$  GSK3 inhibitor (CHIR99021).

### **Cell implantation and *in vivo* imaging**

RNU rats (males, 5-6 weeks old) were purchased from Charles River and housed in individually ventilated cages under a 12h light/dark cycle, with *ad libitum* access to standard food and water. All animal experiments were performed under a licence granted through the UK Animals (Scientific Procedures) Act 1986 and were approved by the University of Liverpool ethics committee. All applicable institutional and/or national guidelines for the care and use of animals were followed. All procedures (surgical administration of cells and imaging) were carried out under isoflurane anaesthesia.

Single-cell suspensions prepared in Hanks' Balanced Salt Solution were implanted stereotactically into the left and right hemispheres of the rats' brains. Using bregma as a

1 reference, the skull was drilled at 0 mm anteroposterior and +/- 1.5 mm mediolateral, with each  
2 hemisphere receiving two deposits of cells at a depth of -5.0 and -4.3 mm from dura. Each  
3 deposit contained  $75 \times 10^3$  cells in 0.75  $\mu\text{L}$  of PBS, delivered with a microsyringe connected to  
4 an infusion pump. Rats were divided into three different experimental groups as outlined in  
5  
6  
7  
8  
9  
10 Table 1.

11  
12  
13 BLI was carried out with an IVIS spectrum system (Perkin Elmer). After inducing anaesthesia,  
14 the rats' heads were shaved and the animals received an intraperitoneal injection of luciferin at  
15 a dose of 150 mg/kg body weight. Data was acquired 20 min post administration of the  
16 substrate with a field of view B (6.5 cm), medium binning, f-stop 1 and exposure time  
17 calculated automatically by the acquisition software, up to a maximum of 5 min. All  
18 bioluminescence data was normalised to the acquisition conditions and are displayed as  
19 radiance (photons/s/cm<sup>2</sup>/str).  
20  
21  
22  
23  
24  
25  
26  
27  
28  
29  
30

31 MRI data was acquired with a Bruker Avance III console interfaced to a 9.4T magnet system  
32 (Bruker Biospec 94/20 USR). RF excitation was achieved with an 86 mm resonator and signal  
33 detection with a 4-channel phased array receive-only rat brain coil. Once the injection site was  
34 located using scout images, higher resolution images were acquired with rapid acquisition with  
35 relaxation enhancement (RARE) sequence. Parameters: echo time (TE) = 38 ms, repetition  
36 time (TR) = 2700 ms, RARE factor = 8, number of excitations (NEX) = 8, field of view (FOV)  
37 = 35x35 mm, matrix size = 350x350 pixels, slices = 20, slice thickness = 500  $\mu\text{m}$ .  
38  
39  
40  
41  
42  
43  
44  
45  
46  
47  
48

49 At the experimental endpoint, the rats received an overdose of pentobarbital and were perfused  
50 transcardially with PBS followed by 4% formaldehyde. The brains were harvested, postfixed  
51 with 4% formaldehyde, equilibrated in 30% sucrose and cryosectioned for microscopy  
52 analysis.  
53  
54  
55  
56  
57  
58  
59  
60  
61  
62  
63  
64  
65

## RT-qPCR

1  
2  
3 Cells were washed twice with PBS and a minimum of  $5 \times 10^5$  cells were lysed with TRI Reagent  
4 (Sigma). Total RNA was extracted according to the manufacturer's protocol and a NanoDrop  
5 (Sigma). Total RNA was extracted according to the manufacturer's protocol and a NanoDrop  
6 was used to determine RNA concentration. To synthesise cDNA, RNA was treated with  
7 DNase1 and reverse transcribed using random hexamers (Qiagen) and Superscript III reverse  
8 transcriptase (Invitrogen). PCR was performed on a CFX Connect system (Bio-Rad) using  
9 SYBR Green JumpStart Taq Ready Mix (Sigma). The genes OTX2, FOXA2 and LMX1A were  
10 measured to assess differentiation into DAPCs, with GAPDH being used as a housekeeping  
11 gene. Undifferentiated hESCs were used as a control. Relative expression levels of target genes  
12 between control and experimental samples were calculated using the  $2^{-\Delta\Delta Ct}$  method [13].  
13  
14  
15  
16  
17  
18  
19  
20  
21  
22  
23  
24  
25  
26  
27  
28  
29  
30  
31  
32  
33  
34  
35  
36  
37  
38  
39  
40  
41  
42  
43  
44  
45  
46  
47  
48  
49  
50  
51  
52  
53  
54  
55  
56  
57  
58  
59  
60  
61  
62  
63  
64  
65

Primer sequences are shown in ESM Table 1.

## Immunostaining and histology

66  
67  
68  
69  
70  
71  
72  
73  
74  
75  
76  
77  
78  
79  
80  
81  
82  
83  
84  
85  
86  
87  
88  
89  
90  
91  
92  
93  
94  
95  
96  
97  
98  
99  
100  
101  
102  
103  
104  
105  
106  
107  
108  
109  
110  
111  
112  
113  
114  
115  
116  
117  
118  
119  
120  
121  
122  
123  
124  
125  
126  
127  
128  
129  
130  
131  
132  
133  
134  
135  
136  
137  
138  
139  
140  
141  
142  
143  
144  
145  
146  
147  
148  
149  
150  
151  
152  
153  
154  
155  
156  
157  
158  
159  
160  
161  
162  
163  
164  
165  
166  
167  
168  
169  
170  
171  
172  
173  
174  
175  
176  
177  
178  
179  
180  
181  
182  
183  
184  
185  
186  
187  
188  
189  
190  
191  
192  
193  
194  
195  
196  
197  
198  
199  
200  
201  
202  
203  
204  
205  
206  
207  
208  
209  
210  
211  
212  
213  
214  
215  
216  
217  
218  
219  
220  
221  
222  
223  
224  
225  
226  
227  
228  
229  
230  
231  
232  
233  
234  
235  
236  
237  
238  
239  
240  
241  
242  
243  
244  
245  
246  
247  
248  
249  
250  
251  
252  
253  
254  
255  
256  
257  
258  
259  
260  
261  
262  
263  
264  
265  
266  
267  
268  
269  
270  
271  
272  
273  
274  
275  
276  
277  
278  
279  
280  
281  
282  
283  
284  
285  
286  
287  
288  
289  
290  
291  
292  
293  
294  
295  
296  
297  
298  
299  
300  
301  
302  
303  
304  
305  
306  
307  
308  
309  
310  
311  
312  
313  
314  
315  
316  
317  
318  
319  
320  
321  
322  
323  
324  
325  
326  
327  
328  
329  
330  
331  
332  
333  
334  
335  
336  
337  
338  
339  
340  
341  
342  
343  
344  
345  
346  
347  
348  
349  
350  
351  
352  
353  
354  
355  
356  
357  
358  
359  
360  
361  
362  
363  
364  
365  
366  
367  
368  
369  
370  
371  
372  
373  
374  
375  
376  
377  
378  
379  
380  
381  
382  
383  
384  
385  
386  
387  
388  
389  
390  
391  
392  
393  
394  
395  
396  
397  
398  
399  
400  
401  
402  
403  
404  
405  
406  
407  
408  
409  
410  
411  
412  
413  
414  
415  
416  
417  
418  
419  
420  
421  
422  
423  
424  
425  
426  
427  
428  
429  
430  
431  
432  
433  
434  
435  
436  
437  
438  
439  
440  
441  
442  
443  
444  
445  
446  
447  
448  
449  
450  
451  
452  
453  
454  
455  
456  
457  
458  
459  
460  
461  
462  
463  
464  
465  
466  
467  
468  
469  
470  
471  
472  
473  
474  
475  
476  
477  
478  
479  
480  
481  
482  
483  
484  
485  
486  
487  
488  
489  
490  
491  
492  
493  
494  
495  
496  
497  
498  
499  
500  
501  
502  
503  
504  
505  
506  
507  
508  
509  
510  
511  
512  
513  
514  
515  
516  
517  
518  
519  
520  
521  
522  
523  
524  
525  
526  
527  
528  
529  
530  
531  
532  
533  
534  
535  
536  
537  
538  
539  
540  
541  
542  
543  
544  
545  
546  
547  
548  
549  
550  
551  
552  
553  
554  
555  
556  
557  
558  
559  
560  
561  
562  
563  
564  
565  
566  
567  
568  
569  
570  
571  
572  
573  
574  
575  
576  
577  
578  
579  
580  
581  
582  
583  
584  
585  
586  
587  
588  
589  
590  
591  
592  
593  
594  
595  
596  
597  
598  
599  
600  
601  
602  
603  
604  
605  
606  
607  
608  
609  
610  
611  
612  
613  
614  
615  
616  
617  
618  
619  
620  
621  
622  
623  
624  
625  
626  
627  
628  
629  
630  
631  
632  
633  
634  
635  
636  
637  
638  
639  
640  
641  
642  
643  
644  
645  
646  
647  
648  
649  
650  
651  
652  
653  
654  
655  
656  
657  
658  
659  
660  
661  
662  
663  
664  
665  
666  
667  
668  
669  
670  
671  
672  
673  
674  
675  
676  
677  
678  
679  
680  
681  
682  
683  
684  
685  
686  
687  
688  
689  
690  
691  
692  
693  
694  
695  
696  
697  
698  
699  
700  
701  
702  
703  
704  
705  
706  
707  
708  
709  
710  
711  
712  
713  
714  
715  
716  
717  
718  
719  
720  
721  
722  
723  
724  
725  
726  
727  
728  
729  
730  
731  
732  
733  
734  
735  
736  
737  
738  
739  
740  
741  
742  
743  
744  
745  
746  
747  
748  
749  
750  
751  
752  
753  
754  
755  
756  
757  
758  
759  
760  
761  
762  
763  
764  
765  
766  
767  
768  
769  
770  
771  
772  
773  
774  
775  
776  
777  
778  
779  
780  
781  
782  
783  
784  
785  
786  
787  
788  
789  
790  
791  
792  
793  
794  
795  
796  
797  
798  
799  
800  
801  
802  
803  
804  
805  
806  
807  
808  
809  
810  
811  
812  
813  
814  
815  
816  
817  
818  
819  
820  
821  
822  
823  
824  
825  
826  
827  
828  
829  
830  
831  
832  
833  
834  
835  
836  
837  
838  
839  
840  
841  
842  
843  
844  
845  
846  
847  
848  
849  
850  
851  
852  
853  
854  
855  
856  
857  
858  
859  
860  
861  
862  
863  
864  
865  
866  
867  
868  
869  
870  
871  
872  
873  
874  
875  
876  
877  
878  
879  
880  
881  
882  
883  
884  
885  
886  
887  
888  
889  
890  
891  
892  
893  
894  
895  
896  
897  
898  
899  
900  
901  
902  
903  
904  
905  
906  
907  
908  
909  
910  
911  
912  
913  
914  
915  
916  
917  
918  
919  
920  
921  
922  
923  
924  
925  
926  
927  
928  
929  
930  
931  
932  
933  
934  
935  
936  
937  
938  
939  
940  
941  
942  
943  
944  
945  
946  
947  
948  
949  
950  
951  
952  
953  
954  
955  
956  
957  
958  
959  
960  
961  
962  
963  
964  
965  
966  
967  
968  
969  
970  
971  
972  
973  
974  
975  
976  
977  
978  
979  
980  
981  
982  
983  
984  
985  
986  
987  
988  
989  
990  
991  
992  
993  
994  
995  
996  
997  
998  
999  
1000

Cells were fixed with 4% formaldehyde for 20 min, permeabilised with 0.1% Triton X-100 for 20 min and blocked with 1% bovine serum albumin (BSA) for 30 min. Cryosections (10  $\mu\text{m}$ ) from fixed tissues were permeabilised and blocked as described above. Primary antibodies were diluted in 1:1 Triton X-100:BSA according to the dilution factors in ESM Table 2 and incubated for 24 h at 4°C. Secondary antibodies were diluted 1:1000 in 1:1 Triton X-100:BSA and incubated for 2h at room temperature. For immunofluorescence, cells were counterstained with DAPI. Images were acquired on a 3i spinning disk confocal microscope CSU-X1 (Intelligent Imaging Innovations) and processed with ImageJ [14]. For immunohistochemistry, tissue sections were incubated with 1.4 mM 3,3'-Diaminobenzidine (DAB), 0.01% hydrogen peroxide for 15 min and images were acquired with a Leica DM IL microscope.

## Results

### **hESC labelling does not negatively impact on differentiation towards DAPCs or mature dopaminergic neurons *in vitro***

Flow cytometry analysis of RC17 hESCs 4 days after viral transduction showed that approximately 47% of the population expressed the reporter gene ZsGreen (ESM Fig. 1a, b). After sorting, a pure population of hESCs expressing the reporter was obtained (Fig. 1a, b); herein defined as Fluc-ZsGreen<sup>+</sup> hESCs. Fluc-ZsGreen<sup>+</sup> hESCs maintained expression of ZsGreen over multiple passages and were morphologically indistinguishable from non-transduced cells (Fig. 1a, b). To assess whether the introduction of the reporter affected pluripotency, embryoid bodies (EB) were generated and immunostained for markers of embryonic germ layer derivatives. The presence of GATA6 (endoderm), Brachyury (mesoderm) and Nestin (ectoderm) confirmed that the Fluc-ZsGreen<sup>+</sup> hESCs remained pluripotent (ESM Fig. 1c).

DAPCs were assessed for the co-expression of the key markers FOXA2, LMX1A and OTX2 on day 16 of differentiation. Quantification of mRNA via RT-qPCR revealed significant upregulation of all these markers (Fig. 1c), which was confirmed via immunofluorescence (Fig. 1d). However, fluorescence microscopy also revealed that not all cells expressed ZsGreen after differentiation into DAPCs (Fig. 1d). DAPCs were further differentiated into mature DA neurons and immunostained (differentiation day 50) to detect the classic DA neuron marker, tyrosine hydroxylase (TH). Immunofluorescence demonstrated that the transduced RC17-derived DA neurons expressed TH (Fig. 1e) but ZsGreen was no longer detectable at this differentiation stage.

1  
2  
3  
4  
5  
6  
7  
8  
9  
10  
11  
12  
13  
14  
15  
16  
17  
18  
19  
20  
21  
22  
23  
24  
25  
26  
27  
28  
29  
30  
31  
32  
33  
34  
35  
36  
37  
38  
39  
40  
41  
42  
43  
44  
45  
46  
47  
48  
49  
50  
51  
52  
53  
54  
55  
56  
57  
58  
59  
60  
61  
62  
63  
64  
65

Flow cytometric analysis of DAPCs showed that only 51% of these cells expressed ZsGreen, implying a significant loss of reporter gene expression when compared to undifferentiated hESCs (Fig. 1f), and complete loss once the cells had matured to dopaminergic neurons (DAs) (Fig. 1e). Measurement of the light output (bioluminescence) revealed that the expression of luciferase corresponded to that of ZsGreen; that is, bioluminescence was strong before differentiation (37 p/s/cell), significantly reduced as cells differentiated towards DAPCs (17 p/s/cell) and extremely weak when they became mature DAs (< 1 p/s/cell) (Fig. 1g).

Taken together, these results show that the introduction of the genetic reporter did not affect hESC pluripotency, nor their ability to differentiate to DAPCs and DA neurons. However, reporter gene expression was progressively lost as the cells differentiated towards DA neurons. Despite the reduction in light emission in DAPCs, we reasoned that it would still be possible to detect them in rodents *in vivo*, enabling their tracking and assessment of viability/tumorigenicity in the early post-transplant period, but that it would not be possible to detect the mature DA neurons.

### ***In vivo* imaging reveals absence of DAPC tumorigenicity and long-term intracranial distribution.**

In addition to assessing the ability of BLI and MRI to detect the implanted cells, a further objective of the *in vivo* studies was to investigate whether the presence of either the Fluc-ZsGreen reporter or the MPIOs affected (i) the tumourigenicity of the cells, (ii) the ability of the hESC-derived DAPCs to differentiate into mature DA neurons *in vivo*, or (iii) the immunogenicity of the human cells. To this end, three groups of rats were set up. Group 1, which served as a control group for tumour formation, comprised of three rats that had Fluc-ZsGreen+ hESCs implanted into the right striatum, and unlabelled hESCs into the left striatum

1 (Fig. 2a); Group 2 comprised of six rats that had DAPCs derived from Fluc-ZsGreen+ hESCs  
2 implanted into the right striatum, and unlabelled cells into the left striatum (Fig. 2d); Group 3  
3  
4 comprised 6 rats that had MPIO-labelled hESC-derived DAPCs implanted into the right  
5 striatum, and unlabelled hESC-derived DAPCs implanted into the left striatum (Fig. 4c).  
6  
7  
8  
9

### 10 11 12 13 14 **hESCs and DAPCs follow distinct fates *in vivo*, irrespective of the introduction of a** 15 **reporter gene** 16 17 18 19

20 Optical imaging of animals that received undifferentiated hESCs on the administration day and  
21 on days 14 and 27 post-administration revealed great variability in the bioluminescence signal.  
22 On the administration day, just one of the animals displayed a signal, which was very weak,  
23 suggesting that Fluc expression was not robust enough for sensitive detection in all animals.  
24  
25 Bioluminescence was progressively lost from this rat but detected in a different animal at a  
26 later time point (ESM Fig. 2a).  
27  
28  
29  
30  
31  
32  
33  
34  
35

36 MR imaging of these rats at the experimental endpoint (day 27) displayed a large area  
37 of atypical hyperintense contrast surrounding the injection site, which was present in both brain  
38 hemispheres of all animals (Fig. 2b and ESM Fig. 2b). Histological analysis of the tissue  
39 showed that this area consisted of a large number of tightly packed cells as evidenced by strong  
40 nuclear (haematoxylin) staining in the same area (Fig. 2b), suggesting an abnormal growth of  
41 cells. Immunofluorescence microscopy of these samples revealed that the masses in both  
42 hemispheres consisted of human cells, as evidenced by positive staining for a human specific  
43 nuclear antigen (hNuclei). Interestingly, however, not all cells in the masses that formed in the  
44 right brain hemisphere (Fluc-ZsGreen<sup>+</sup> hESCs) expressed ZsGreen, suggesting that some of the  
45 hESCs lost expression of the reporter (Fig 2c). The hESC-derived masses did not display a  
46 teratoma-like tissue architecture when examined by haematoxylin and eosin staining (data not  
47  
48  
49  
50  
51  
52  
53  
54  
55  
56  
57  
58  
59  
60  
61  
62  
63  
64  
65

1 shown). Instead, many of the cells expressed  $\beta$ -III tubulin, suggesting that transplantation of  
2 these cells in the rat brain promoted differentiation to ectodermal lineages (ESM Fig. 2c). The  
3  
4 growths were also negative for OCT4, confirming that cells had differentiated in the brain  
5 (ESM Fig. 2d). Taken together, these results indicate that undifferentiated hESCs form mass  
6  
7 lesions, irrespective of the introduction of the Fluc-ZsGreen reporter.  
8  
9

10  
11  
12 For rats implanted with DAPCs (group 2) (Fig. 2d), 4 of 6 animals displayed a  
13 bioluminescence signal on the administration day (Fig. 2e and ESM Fig. 3a), which was not  
14  
15 detectable at the subsequent imaging points (days 14, 28, 56 and 91). In contrast to hESCs,  
16  
17 administration of DAPCs resulted in no abnormal MR contrast at the experimental endpoint  
18  
19 (day 91, Fig. 2f), with all animals exhibiting normal brain structures and the needle track being  
20  
21 the only remarkable feature.  
22  
23  
24  
25  
26  
27

28  
29 Human cells were still present at the injection site in both hemispheres, as evidenced  
30  
31 by hNuclei positivity (Fig. 3a). Importantly, the areas containing human cells were also positive  
32  
33 for TH, suggesting maturation of some DAPCs in the rats' brains within the experimental  
34  
35 period (91 days). Not all human cells robustly expressed TH, likely because a period of >20  
36  
37 weeks is necessary for the maturation of all DAPCs. The injection sites were also positive for  
38  
39 a human-specific NCAM (hNCAM) antigen (Fig. 3b), providing further evidence that human  
40  
41 cells had integrated with the rat brain and displayed neural lineage commitment, irrespective  
42  
43 of whether they had been genetically modified.  
44  
45  
46  
47  
48  
49  
50  
51  
52

### 53 **MPIO labelling enables assessment of the intracranial distribution of implanted cells**

54  
55

56 Flow cytometry analysis of MPIO-labelled DAPCs suggested that approximately 72% of  
57  
58 DAPCs were labelled with the particles, as evidenced by yellow fluorescence originating from  
59  
60  
61  
62  
63  
64  
65

1  
2  
3  
4  
5  
6  
7  
8  
9  
10  
11  
12  
13  
14  
15  
16  
17  
18  
19  
20  
21  
22  
23  
24  
25  
26  
27  
28  
29  
30  
31  
32  
33  
34  
35  
36  
37  
38  
39  
40  
41  
42  
43  
44  
45  
46  
47  
48  
49  
50  
51  
52  
53  
54  
55  
56  
57  
58  
59  
60  
61  
62  
63  
64  
65

MPIOs (Fig. 4a). We also detected a shift in the side scatter of DAPCs after labelling with MPIOs, providing further evidence for the internalisation of the particles (Fig. 4b).

Rats implanted with MPIO-labelled DAPCs (group 3) (Fig. 4c) were imaged only via MR, as neither of the hemispheres received cells with the genetic reporter. Monitoring of this group for up to 4 months post implantation confirmed that DAPC implantation does not lead to tumour formation, with all rats displaying normal brain structures at all time points. In 5 out of 6 rats, hypointense contrast was seen in the right brain hemisphere (Fig. 4d and ESM Fig. 3b). This was an expected consequence of the MPIO labelling, which enabled us to monitor the delivery and intracranial distribution of DAPCs. Remarkably, the distribution of the administered DAPCs appears to remain stable throughout the 4 months that the animals were monitored for, with no obvious change in the area with hypointense contrast, suggesting that the DAPCs were confined to the areas into which they were initially deposited. In one rat, no hypointense contrast was observed in the target area. Further analysis of the scans revealed that for this animal, the needle had been inserted at an angle, with the cells delivered to the ventricle leading to them becoming lodged at a different anatomical location (ESM Fig. 3c).

As observed before, immunofluorescence staining at the injection sites confirmed the presence of human cells that expressed TH, reinforcing the point that these cells were able to integrate within the rat brain and differentiated into mature DAs, irrespective of the MPIO labelling (Fig. 4e). In the right hemisphere, MPIOs were found in the same areas as the administered human cells and appeared to localise to perinuclear regions.

### **Intense staining for GFAP is observed surrounding the human cell implants**

1 A previous study showed that the implantation of Fluc+ hESC-derived neural stem cells into  
2 the mouse striatum caused marked glial reaction in the host brain, as evidenced by intense  
3 immunostaining for glial fibrillary acidic protein (GFAP), a marker of reactive astrocytes<sup>11</sup>. To  
4 investigate whether Fluc-ZsGreen or MPIOs contributed to this reaction, sections from group  
5 2 and group 3 rats were immunostained for GFAP. Qualitative analysis showed an increase in  
6 GFAP staining around the human implants, but no differences in staining intensity were  
7 observed around implants comprising unlabelled human cells or MPIO-labelled cells (Fig. 5a  
8 and ESM Fig. 4a) and cells derived from Fluc-ZsGreen+ hESCs (Fig. 5b and ESM Fig. 4b).  
9 Consistent with the expression profile of ZsGreen in mature DA neurons *in vitro* (Fig. 1e),  
10 expression of ZsGreen in brain sections was barely detectable (Fig. 5b and ESM Fig. 4b).  
11  
12  
13  
14  
15  
16  
17  
18  
19  
20  
21  
22  
23  
24  
25  
26  
27

## 28 Discussion

29  
30  
31 Our study assessed the effectiveness of BLI and MR imaging to monitor the tumourigenicity,  
32 viability and intracranial biodistribution of hESC-derived DAPCs following stereotactic  
33 injection into the rat striatum. In most animals, BLI could only detect Fluc-ZsGreen<sup>+</sup> cells  
34 shortly after administration and was not effective for monitoring tumourigenicity and cell  
35 viability in the longer-term. MR imaging, on the other hand, could detect tumours arising from  
36 undifferentiated hESCs and could monitor the intracranial biodistribution of MPIO-labelled  
37 hESC-derived DAPCs over the full time-course of our experiments.  
38  
39  
40  
41  
42  
43  
44  
45  
46  
47  
48  
49

50 The inability to detect cells with BLI likely resulted from a number of factors. First, at  
51 the initial imaging session, the rats were only 6 weeks old. During the intervening two weeks  
52 before the next imaging session, the rats grew considerably and became more pigmented (see  
53 ESM Fig. 3a), causing the intensity of the emitted light to be reduced; this likely explains why  
54 after day 1, bioluminescence could only be detected in a rat that had developed a large Fluc-

1 ZsGreen<sup>+</sup> hESC-derived mass (ESM Fig. 2a, rat 3). Bernau *et al* found that Fluc<sup>+</sup> human foetal  
2 neuronal progenitors implanted into the rat striatum could be imaged with BLI for 3 months  
3  
4 [15]. However, they implanted  $9 \times 10^5$  Fluc<sup>+</sup> cells into the left hemisphere compared with only  
5  
6  $1.5 \times 10^5$  cells in our study. An additional problem was that in comparison with undifferentiated  
7  
8 hESCs, we found that the expression levels of the reporter genes decreased by ~50% in Fluc-  
9  
10 ZsGreen<sup>+</sup> hESC-derived DAPCs, and could not be detected at all in the mature DA neurons. It  
11  
12 is well recognised that ESC differentiation is accompanied by increased levels of DNA  
13  
14 methylation, leading to gene silencing, and that the pattern of silencing is cell type specific  
15  
16 [16]. The choice of promoter also affects the extent of silencing. A previous study comparing  
17  
18 the activity of five constitutive promoters, EF1 $\alpha$ , human  $\beta$ -actin (ACTB), cytomegalovirus  
19  
20 (CMV), phosphoglycerate kinase (PGK) and ubiquitinC (UbC) in differentiating hESCs,  
21  
22 reported that EF1 $\alpha$  was the most stable, with expression levels in EBs being reduced to ~50%  
23  
24 of those in undifferentiated hESCs [17]. Our observation that Fluc-ZsGreen expression was  
25  
26 undetectable in the mature DA neurons, both *in vitro* and *in vivo*, was unexpected. Tennstaedt  
27  
28 *et al* have shown that a EF1 $\alpha$ :Fluc-GFP<sup>+</sup> neural stem cell line derived from hESCs could be  
29  
30 detected with BLI for 6 weeks following injection into the mouse brain without any noticeable  
31  
32 decrease in bioluminescence intensity [18]. However, the neural stem cells used in the  
33  
34 Tennstaedt study have a different phenotype to hESC-derived DAPCs and there is no evidence  
35  
36 that they differentiate into the DA lineage [18]. Likewise, there is no evidence that the Fluc<sup>+</sup>  
37  
38 human foetal neuron progenitors used in the aforementioned Bernau *et al* study differentiate  
39  
40 into the DA lineage in the rat brain [15]. Indeed, as far as we are aware, there are no studies  
41  
42 that show Fluc expression in hESC-derived DA neurons *in vivo* when Fluc is under the control  
43  
44 of a constitutive promoter. In future studies, a cell type-specific promoter, such as FOXA2,  
45  
46 which is expressed in both DAPCs and mature DA neurons [19], could prove more effective  
47  
48 than the EF1 $\alpha$  promoter for monitoring viability longitudinally, especially if used with the  
49  
50  
51  
52  
53  
54  
55  
56  
57  
58  
59  
60  
61  
62  
63  
64  
65

1 highly sensitive AkaLuc luciferase in combination with the substrate Akalumine [20].  
2 However, one advantage of our system is that the loss of signal is due to differentiation. This  
3 could be used to show that the grafted cells have indeed followed the correct pathway post  
4 implantation rather than dedifferentiated back into an ESC-like phenotype.  
5  
6  
7  
8  
9

10 Four weeks after implantation of undifferentiated hESCs, MR imaging could detect a  
11 cell mass in both cerebral hemispheres, irrespective of whether the cells had been transduced  
12 with the Fluc-ZsGreen reporter (ESM Fig. 2b). However, no cell masses were detected at any  
13 time point following administration of hESC-derived DAPCs, suggesting that in contrast to the  
14 undifferentiated hESCs, the DAPCs are non-tumourigenic. Cells labelled with MPIOs could  
15 be detected at all time points using longitudinal MR imaging. In addition, we found that the  
16 cells remained at the injection site and did not appear to migrate to other brain regions. From a  
17 safety perspective, the lack of migration is important to prevent cells integrating into intact  
18 neural circuits causing side effects (e.g. epilepsy) [21].  
19  
20  
21  
22  
23  
24  
25  
26  
27  
28  
29  
30  
31  
32

33 Previous studies have shown that labelling cells with iron oxide nanoparticles can  
34 inhibit differentiation to specific lineages [22-23]. In our study, we did not find any evidence  
35 that the bicistronic Fluc-ZsGreen reporter or the MPIOs inhibited the differentiation of hESC-  
36 derived DAPCs into TH+ DA neurons. The final aim of our study was to investigate whether  
37 the reporter or the MPIOs increased glial reactivity to the grafted cells. It is known that the  
38 implantation of cells into the brain induces a glial response [24], as evidenced by increased  
39 numbers of reactive GFAP+ astrocytes surrounding the grafts [10]. Transplantation of both  
40 labelled and unlabelled DAPCs elicited a marked glial reaction at the injection site, as expected.  
41 However, there was no notable difference in the scale of glial response, suggesting that neither  
42 Fluc-ZsGreen nor MPIOs increased the glial reaction to the DAPCs [25].  
43  
44  
45  
46  
47  
48  
49  
50  
51  
52  
53  
54  
55  
56  
57  
58  
59  
60  
61  
62  
63  
64  
65

## Conclusions

In summary, we have demonstrated that hESC-derived DAPCs can be labelled with luminescence and contrast-enhancing reporters for *in vivo* cell tracking. Following intracranial transplantation in the rat striatum, our findings support the safe implementation of DAPC-derived therapies for the treatment of PD.

## Acknowledgements

We gratefully acknowledge support by the Medical Research Council, Engineering and Physical Sciences Research Council and Biotechnology and Biological Sciences Research Council funded UK Regenerative Medicine Platform “Safety and Efficacy, focussing on Imaging Technologies Hub” (MR/K026739/1) and Pluripotent Stem Cell Hub. All *in vivo* imaging was carried out in the Centre for Preclinical Imaging, University of Liverpool. R.A.B is an NIHR Senior Investigator.

## Conflict of Interest

The authors declare that they have no conflict of interest.

## References

1. Grealish S, Diguët E, Kirkeby A, et al. (2014) Human ESC-Derived Dopamine Neurons Show Similar Preclinical Efficacy and Potency to Fetal Neurons when Grafted in a Rat Model of Parkinson's Disease. *Cell Stem Cell* 15:653-665.
2. Kriks S, Shim JW, Piao JH, et al. (2011) Dopamine neurons derived from human ES cells efficiently engraft in animal models of Parkinson's disease. *Nature* 480:547-U177.

- 1  
2  
3  
4  
5  
6  
7  
8  
9  
10  
11  
12  
13  
14  
15  
16  
17  
18  
19  
20  
21  
22  
23  
24  
25  
26  
27  
28  
29  
30  
31  
32  
33  
34  
35  
36  
37  
38  
39  
40  
41  
42  
43  
44  
45  
46  
47  
48  
49  
50  
51  
52  
53  
54  
55  
56  
57  
58  
59  
60  
61  
62  
63  
64  
65
3. Heslop JA, Hammond TG, Santeramo I, et al. (2015) Concise Review: Workshop Review: Understanding and Assessing the Risks of Stem Cell-Based Therapies. *Stem Cells Transl Med* 4:389-400.
4. Scarfe L, Taylor A, Sharkey J, et al. (2018) Non-invasive imaging reveals conditions that impact distribution and persistence of cells after in vivo administration. *Stem Cell Res Ther* 9.
5. Mezzanotte L, Iljas JD, Que I, et al. (2017) Optimized Longitudinal Monitoring of Stem Cell Grafts in Mouse Brain Using a Novel Bioluminescent/Near Infrared Fluorescent Fusion Reporter. *Cell Transplant* 26:1878-1889.
6. Tennstaedt A, Aswendt M, Adamczak J, Hoehn M (2013) Noninvasive Multimodal Imaging of Stem Cell Transplants in the Brain Using Bioluminescence Imaging and Magnetic Resonance Imaging. In *Imaging and Tracking Stem Cells: Methods and Protocols*, Ed. Turksen K. pp 153-166.
7. Jost SC, Collins L, Travers S, Piwnica-Worms D, Garbow JR (2009) Measuring Brain Tumor Growth: Combined Bioluminescence Imaging-Magnetic Resonance Imaging Strategy. *Mol Imaging* 8:245-253.
8. Taylor A, Herrmann A, Moss D, et al. (2014) Assessing the Efficacy of Nano- and Micro-Sized Magnetic Particles as Contrast Agents for MRI Cell Tracking. *PLoS One* 9.
9. Galisova A, Herynek V, Swider E, et al. (2019) A Trimodal Imaging Platform for Tracking Viable Transplanted Pancreatic Islets In Vivo: F-19 MR, Fluorescence, and Bioluminescence Imaging. *Mol Imaging Biol* 21:454-464.
10. Tennstaedt A, Mastropietro A, Nelles M, Beyrau A, Hoehn M (2015) In Vivo Fate Imaging of Intracerebral Stem Cell Grafts in Mouse Brain. *PLoS One* 10.

- 1  
2  
3  
4  
5  
6  
7  
8  
9  
10  
11  
12  
13  
14  
15  
16  
17  
18  
19  
20  
21  
22  
23  
24  
25  
26  
27  
28  
29  
30  
31  
32  
33  
34  
35  
36  
37  
38  
39  
40  
41  
42  
43  
44  
45  
46  
47  
48  
49  
50  
51  
52  
53  
54  
55  
56  
57  
58  
59  
60  
61  
62  
63  
64  
65
11. Taylor A, Sharkey J, Plagge A, Wilm B, Murray P (2018) Multicolour In Vivo Bioluminescence Imaging Using a NanoLuc-Based BRET Reporter in Combination with Firefly Luciferase. *Contrast Media Mol I*.
12. Nolbrant S, Heuer A, Parmar M, Kirkeby A (2017) Generation of high-purity human ventral midbrain dopaminergic progenitors for in vitro maturation and intracerebral transplantation. *Nat Protoc* 12:1962-1979.
13. Livak KJ, Schmittgen TD (2001) Analysis of relative gene expression data using real-time quantitative PCR and the  $2^{-\Delta\Delta C_T}$  method. *Methods* 25:402-408.
14. Schneider CA, Rasband WS, Eliceiri KW (2012) NIH Image to ImageJ: 25 years of image analysis. *Nat Methods* 9:671-675.
15. Bernau K, Lewis CM, Petelinsek AM, et al. (2014) In vivo tracking of human neural progenitor cells in the rat brain using bioluminescence imaging. *J Neurosci Methods* 228:67-78.
16. Suelves M, Carrio E, Nunez-Alvarez Y, Peinado MA (2016) DNA methylation dynamics in cellular commitment and differentiation. *Brief Funct Genomics* 15:443-453.
17. Norrman K, Fischer Y, Bonnamy B, Sand FW, Ravassard P, Semb H (2010) Quantitative Comparison of Constitutive Promoters in Human ES cells. *PLoS One* 5.
18. Tennstaedt A, Aswendt M, Adamczak J, et al. (2015) Human neural stem cell intracerebral grafts show spontaneous early neuronal differentiation after several weeks. *Biomaterials* 44:143-154.
19. Domanskyi A, Alter H, Vogt MA, Gass P, Vinnikov IA (2014) Transcription factors Foxa1 and Foxa2 are required for adult dopamine neurons maintenance. *Front Cell Neurosci* 8.
20. Iwano S, Sugiyama M, Hama H, et al. (2018) Single-cell bioluminescence imaging of deep tissue in freely moving animals. *Science* 359:935-939.

- 1  
2  
3  
4  
5  
6  
7  
8  
9  
10  
11  
12  
13  
14  
15  
16  
17  
18  
19  
20  
21  
22  
23  
24  
25  
26  
27  
28  
29  
30  
31  
32  
33  
34  
35  
36  
37  
38  
39  
40  
41  
42  
43  
44  
45  
46  
47  
48  
49  
50  
51  
52  
53  
54  
55  
56  
57  
58  
59  
60  
61  
62  
63  
64  
65
21. Wijeyekoon R, Barker RA (2009) Cell replacement therapy for Parkinson's disease. *Biochim Biophys Acta, Mol Basis Dis* 1792:688-702.
22. Kostura L, Kraitchman DL, Mackay AM, Pittenger MF, Bulte JWM (2004) Feridex labeling of mesenchymal stem cells inhibits chondrogenesis but not adipogenesis or osteogenesis. *NMR Biomed* 17:513-517.
23. Kolecka MA, Arnhold S, Schmidt M, et al. (2017) Behaviour of adipose-derived canine mesenchymal stem cells after superparamagnetic iron oxide nanoparticles labelling for magnetic resonance imaging. *BMC Vet Res* 13.
24. Cicchetti F, Barker RA (2014) The glial response to intracerebrally delivered therapies for neurodegenerative disorders: is this a critical issue? *Front Pharmacol* 5.
25. Purushothuman S, Marotte L, Stowe S, Johnstone DM, Stone J (2013) The Response of Cerebral Cortex to Haemorrhagic Damage: Experimental Evidence from a Penetrating Injury Model. *PLoS One* 8.

## Figure Legends

1  
2  
3 **Figure 1. Effect and stability of the Fluc-ZsGreen reporter gene in hESCs.** (a) Phase  
4 contrast and fluorescence microscopy of control and Fluc-ZsGreen<sup>+</sup> hESCs. Cells were imaged  
5  
6 3 passages post sorting. (b) ZsGreen expression, as measured via flow cytometry, of control  
7  
8 and sorted hESCs. The green fluorescence of sorted cells is stable for several passages. (c)  
9  
10 Expression of OTX2, FOXA2 and LMX1 in DAPCs obtained from Fluc-ZsGreen<sup>+</sup> hESCs. (d,  
11  
12  
13 e) Fluorescence microscopy of DAPCs and DAs obtained from Fluc-ZsGreen<sup>+</sup> hESCs  
14  
15 (differentiation days 15 and 50 respectively). Cells were immunostained for OTX2, FOXA2,  
16  
17 LMX1A and TH. (f) Flow cytometry shows that differentiation into DAPCs reduces ZsGreen  
18  
19 expression (approx. 47% of the cells expressing the construct). (g) BLI of different numbers of  
20  
21 Fluc-ZsGreen<sup>+</sup> hESCs, DAPCs, and mDAs and the corresponding photon flux. Data are  
22  
23 representative of three independent experiments. Error bars represent SD and the solid line the  
24  
25 linear fit of the data. Scale bars in micrographs correspond to 100  $\mu$ m.  
26  
27  
28  
29  
30  
31  
32  
33  
34  
35

36 **Figure 2. Long-term fate of hESCs and DAPCs.** (a) Schematic of injection and experimental  
37  
38 timeline of hESC administration and imaging (b) Representative RARE MRI scan (day 27)  
39  
40 and corresponding histological section (H&E staining) of a rat that received undifferentiated  
41  
42 hESCs (left hemisphere: non-transduced, right hemisphere: Fluc-ZsGreen<sup>+</sup>). Both sides display  
43  
44 a large area of hyperintense contrast at the injection site (arrowheads) which was confirmed to  
45  
46 correspond to tightly packed cell nuclei via histology. (c) Fluorescence microscopy of areas of  
47  
48 abnormal growth in the right hemisphere. In all cases the growth corresponded to cells of  
49  
50 human origin, as evidenced by expression of a human nuclear antigen. The level of ZsGreen  
51  
52 expression was heterogeneous within the growths, with areas of strong expression (top) and  
53  
54 areas where ZsGreen was lost (bottom). Scale bar = 50  $\mu$ m (d) Schematic of injection and  
55  
56  
57  
58  
59  
60  
61  
62  
63  
64  
65

1 experimental timeline of DAPC administration and imaging (e) BLI of two of the six rats that  
2 received DAPCs as imaged on days 1, 14 and 91. Most, but not all rats displayed a signal on  
3 the injection day, but this was lost by day 14 and no signal was seen up at any other time points.  
4  
5 Left panel is representative of rats that displayed signal on day 1, and the right panel  
6  
7 representative of rats that did not display a signal in any of the days. Data for the other rats and  
8  
9 time points are shown in the SI. Note that this rat strain can display cycles of thin hair growth,  
10  
11 as seen in some images. (f) RARE MRI scans (day 90) of all 6 rats that received DAPCs (left  
12  
13 hemisphere: non-transduced, right hemisphere: Fluc-ZsGreen<sup>+</sup>). No abnormal features are  
14  
15 seen, apart from the needle track that is still visible in some animals (indicated arrowheads in  
16  
17 the first rat only).  
18  
19  
20  
21  
22  
23  
24  
25  
26  
27

28 **Figure 3. DAPC integration with the rat brain.** (a) Immunofluorescence microscopy of the  
29 injection sites (left hemisphere: non-transduced, right hemisphere: Fluc-ZsGreen<sup>+</sup>). Cells  
30 express a human nuclear antigen, showing that the DAPCs survived in the rats' brains and  
31 expressed TH, suggesting that they matured into DAs. Arrowhead indicates a human cell  
32 strongly expressing TH. (b) Immunofluorescence of a similar area but using an antibody  
33 against human NCAM as a means to confirm the human origin of the cells. Scale bars  
34 correspond to 50  $\mu\text{m}$ .  
35  
36  
37  
38  
39  
40  
41  
42  
43  
44  
45  
46  
47  
48

49 **Figure 4. MPIO tracking of DAPCs in the rat brain.** (a) Yellow fluorescence of unlabelled  
50 and MPIO-labelled DAPCs. (b) Forward vs. side-scatter plot of unlabelled and MPIO-labelled  
51 DAPCs. (c) Schematic of injection and experimental timeline of DAPC administration and  
52 magnetic resonance imaging (d) Representative RARE MRI scans of a rat that received MPIO-  
53 labelled DAPC (left hemisphere: unlabelled, right hemisphere: labelled) as imaged on day 1,  
54  
55  
56  
57  
58  
59  
60  
61  
62  
63  
64  
65

1  
2  
3  
4  
5  
6  
7  
8  
9  
10  
11  
12  
13  
14  
15  
16  
17  
18  
19  
20  
21  
22  
23  
24  
25  
26  
27  
28  
29  
30  
31  
32  
33  
34  
35  
36  
37  
38  
39  
40  
41  
42  
43  
44  
45  
46  
47  
48  
49  
50  
51  
52  
53  
54  
55  
56  
57  
58  
59  
60  
61  
62  
63  
64  
65

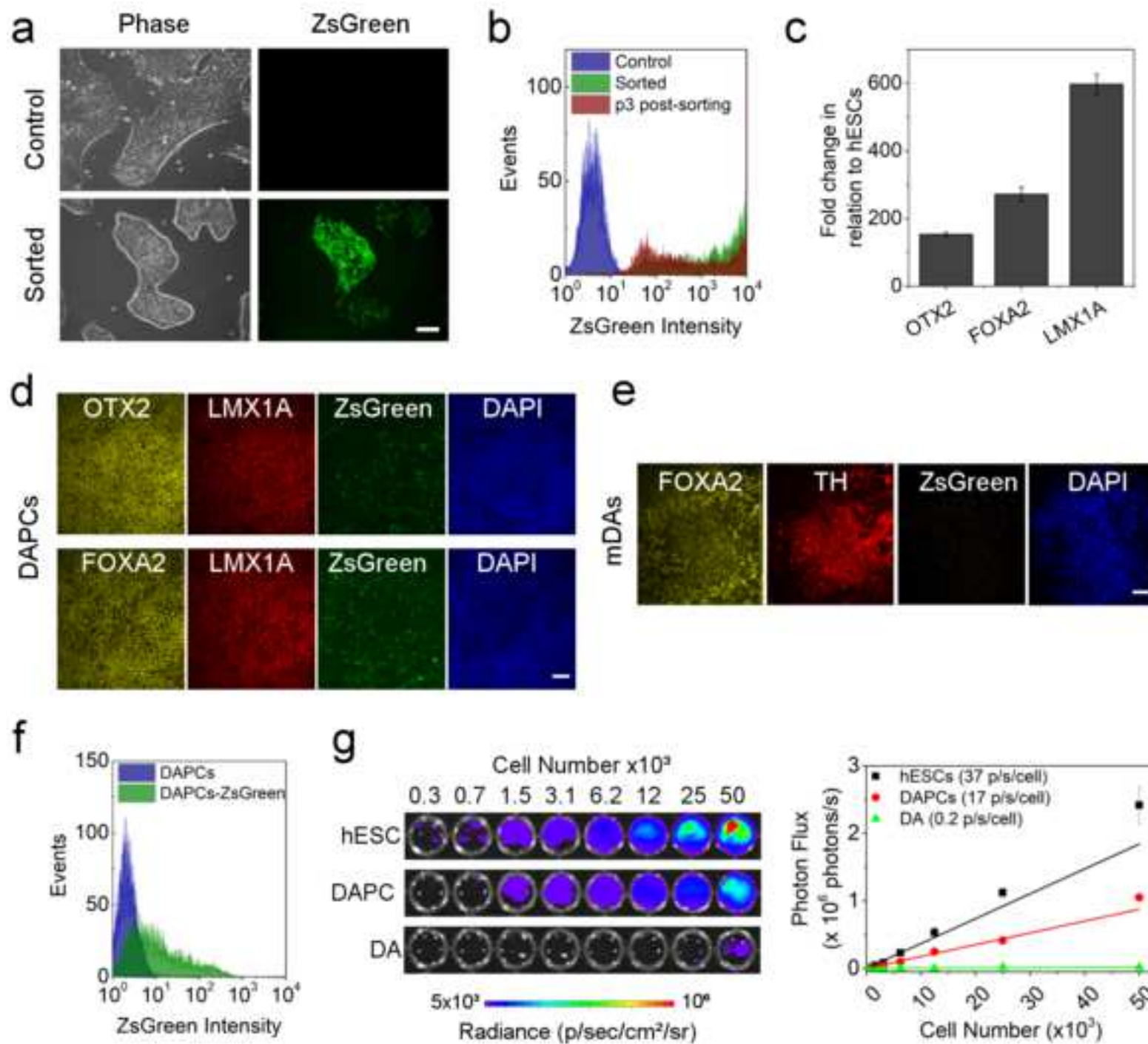
14, 28, 42, 70 and 126 post-administration. Hypointense contrast, indicative of a reduction in relaxation time as caused by MPIO labelling, is seen in the right hemisphere throughout the experimental period (indicated with an arrowhead in the first image). No abnormal growth is observed in either of the hemispheres. **(e)** Immunofluorescence microscopy of the injection sites. Cells express human NCAM, showing that MPIO-labelled DAPCs survived in the rats' brains and TH, suggesting that DAPCs matured into DAs. MPIO-specific fluorescence is only seen in the right hemisphere, and tends to be localised to near the cell nuclei. Note that the MPIO fluorophore, Suncoast Yellow, is excited at 405 nm and bleeds into the DAPI channel. Scale bar = 50  $\mu\text{m}$ .

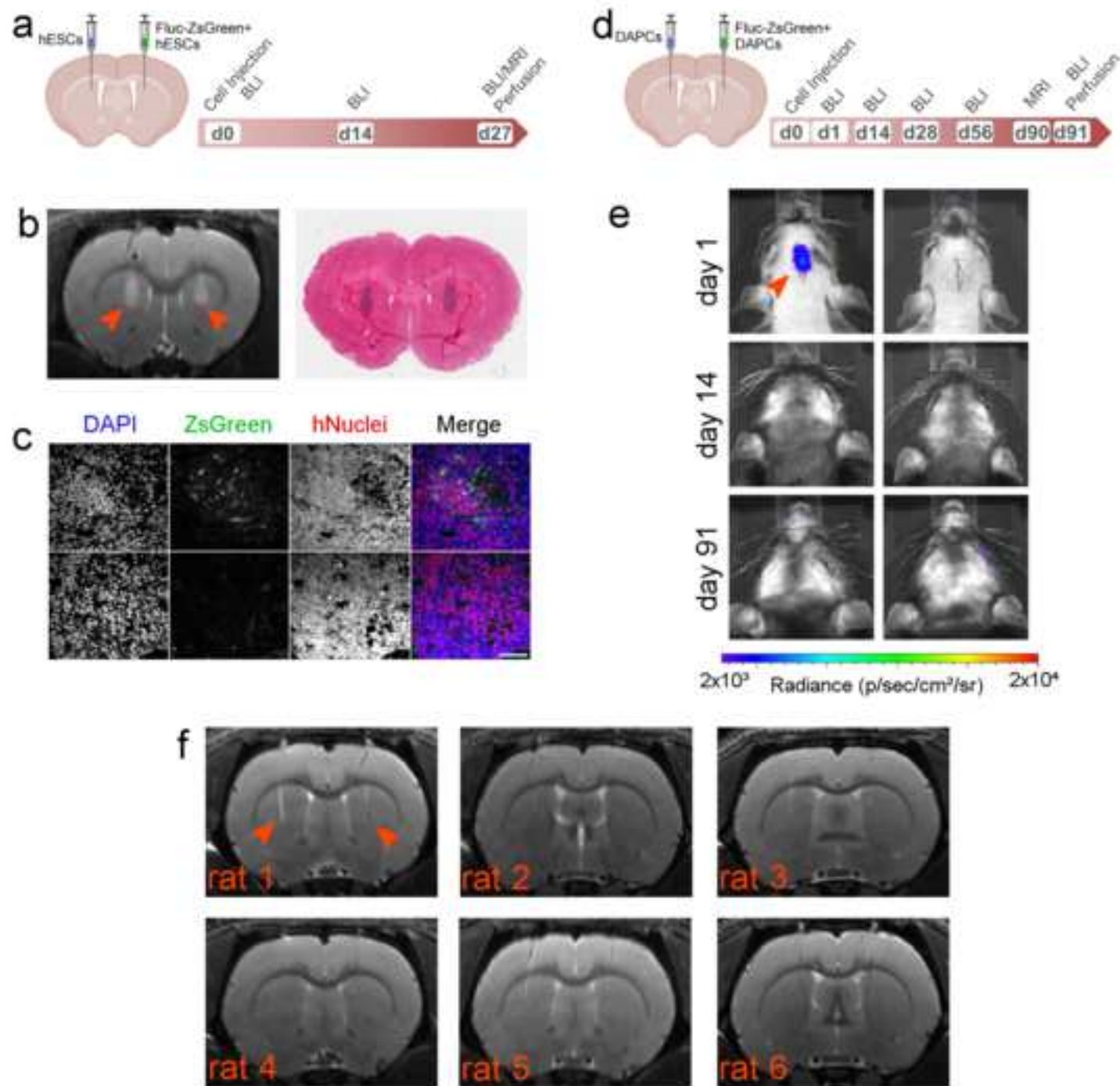
**Figure 5. Glial reaction at the injection sites.** **(a)** Immunofluorescence microscopy of brains from rats that received MPIO-labelled DAPCs (left hemisphere: unlabelled; right hemisphere: labelled). The presence of human cells is identified with hNCAM staining, and the intensity of GFAP staining is stronger in these areas. MPIOs are only seen in the right hemisphere. **(b)** Immunofluorescence microscopy of brains from rats that received Fluc-ZsGreen+ DAPCs (left hemisphere: untransduced control cells; right hemisphere Fluc-ZsGreen+ cells). Scale bars correspond to 100  $\mu\text{m}$ .

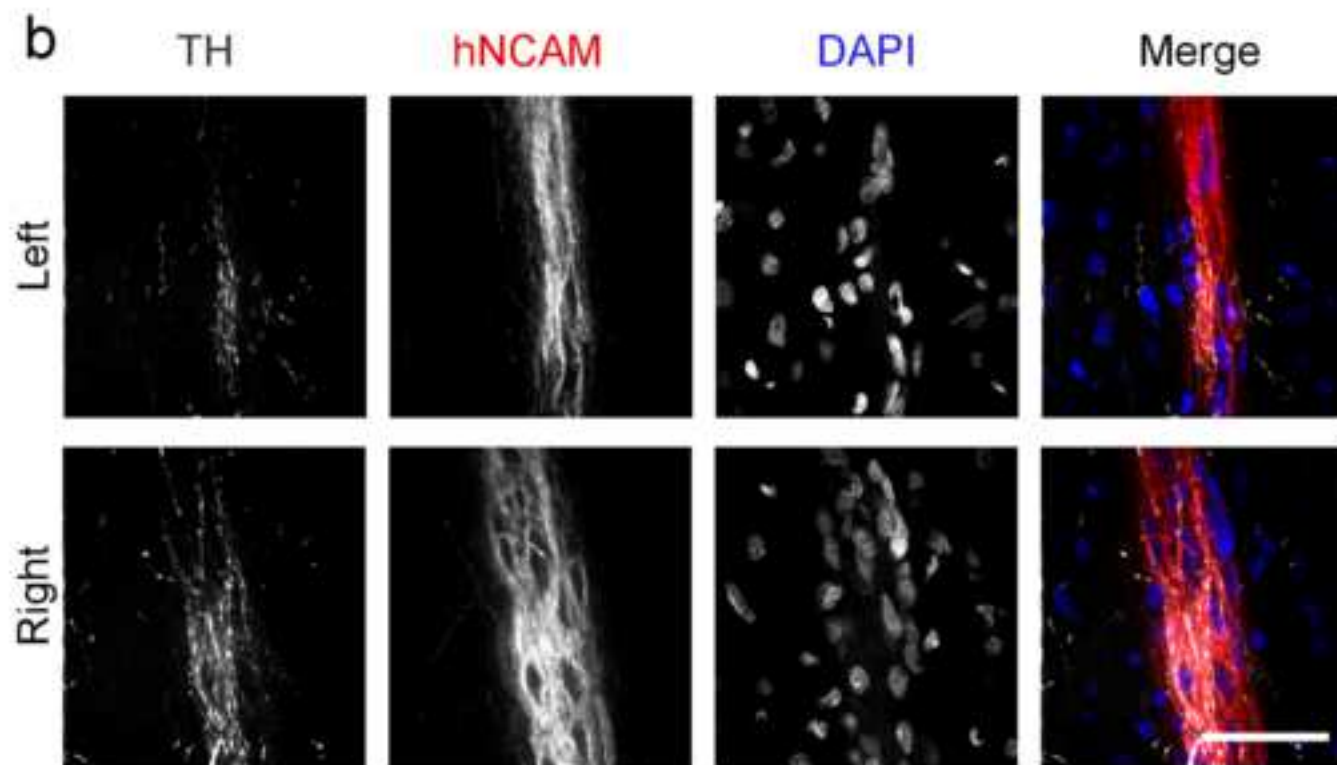
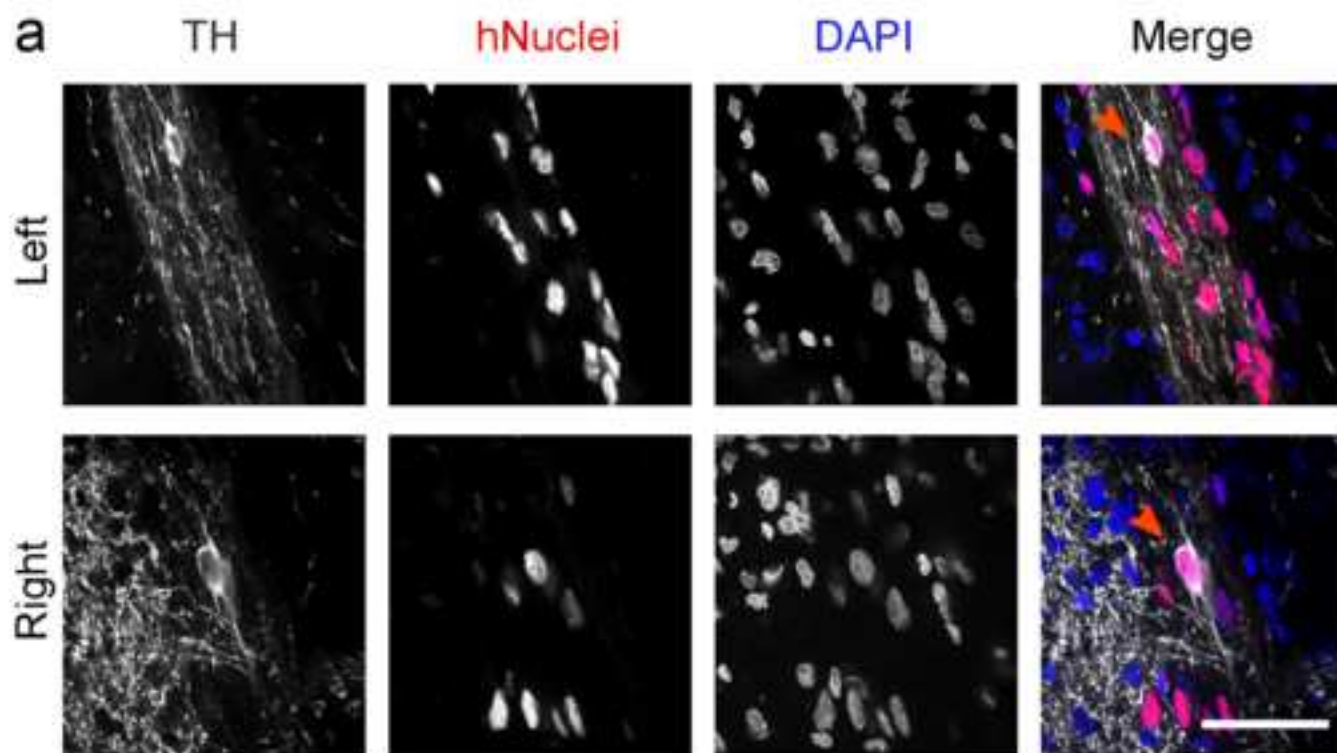
## Tables

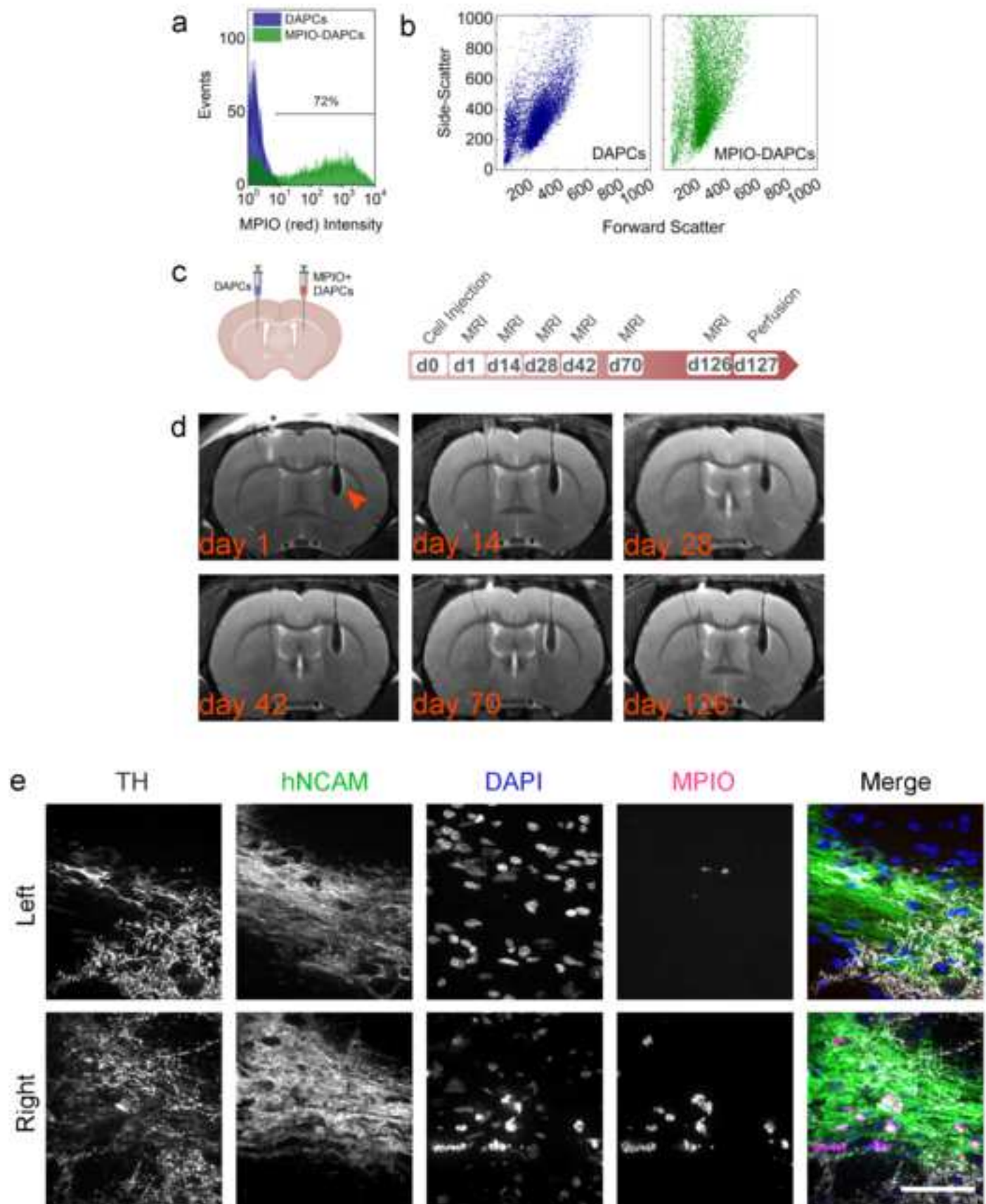
**Table 1.** Description of the experimental groups.

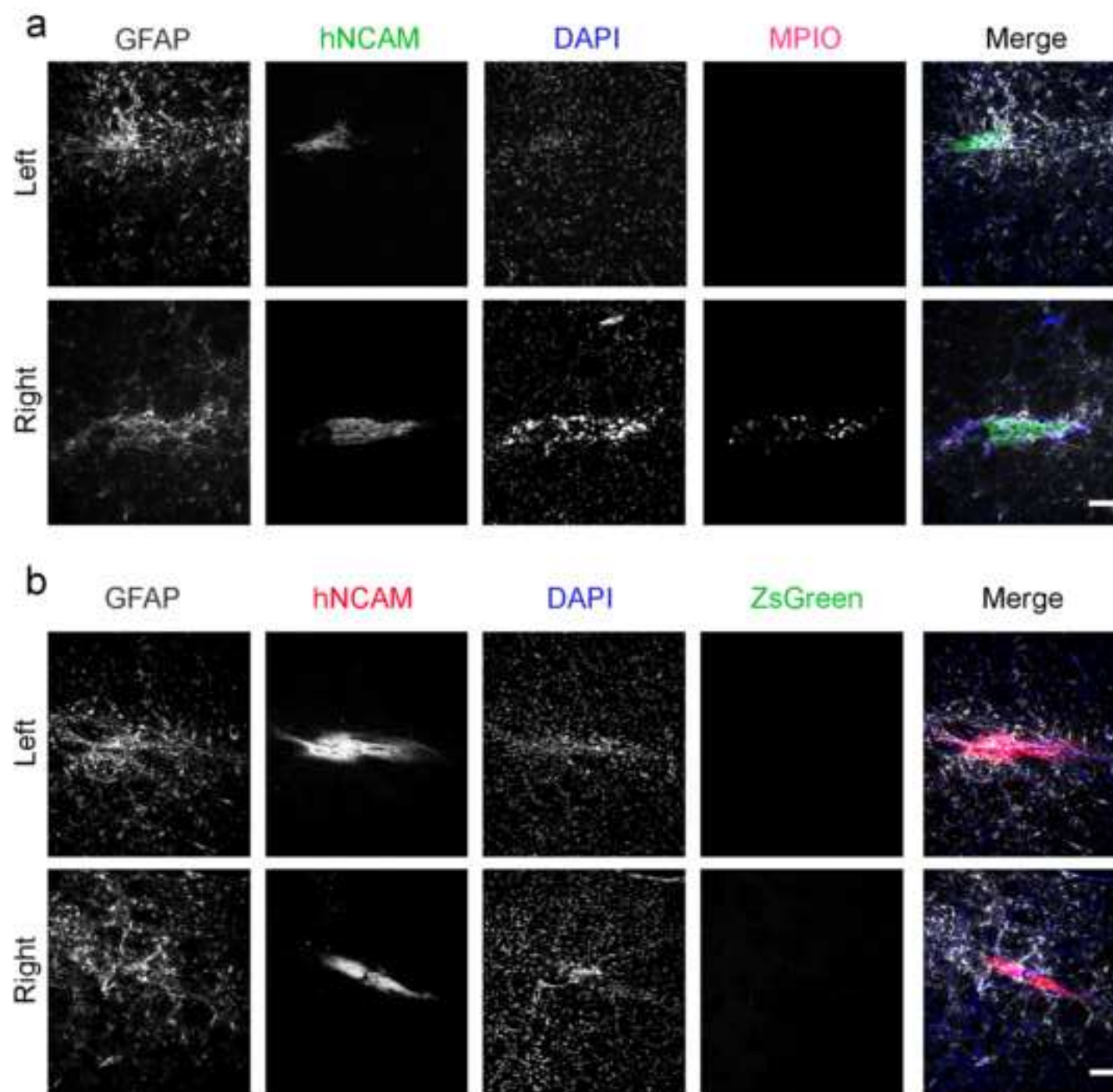
<b>Group</b>	<b>Cells implanted in left hemisphere</b>	<b>Cells implanted in right hemisphere</b>	<b>Number of animals</b>	<b>Endpoint</b>
<b>1</b>	Undifferentiated hESCs	Undifferentiated hESCs (Fluc-ZsGreen <sup>+</sup> )	3	day 27
<b>2</b>	DAPCs	DAPCs (Fluc-ZsGreen <sup>+</sup> )	6	day 91
<b>3</b>	DAPCs	DAPCs (MPIO-labelled)	6	day 127













Click here to access/download

**Supplementary Material**

Mousavinejad\_et\_al\_Supplementary\_Information\_revised.docx



## Response to reviewers' comments

Re: “Assessing human embryonic stem cell-derived dopaminergic neuron progenitor transplants using non-invasive imaging techniques” by Mousavinejad *et al.* 2020

Reviewer #1: In this study the authors trying to show the longevity and fate of implanted hESC before and after differentiated into DAPC and DA in the striatum of Rat by longitudinal assessment. They used cells labelled with luciferase (for bioluminescence imaging) and micro-sized iron oxide (MPIO) particles (for MR-Imaging) as reporters for dual imaging in vivo. The comparison of cell viability before and after differentiation into DAPC and DA compared to hESC were systematically evaluated in vitro and in vivo in rat after implantation. They evaluated the growth, differentiation and teratoma formation several weeks after implantation of hESC and DAPC and observed that there is no big difference between the cells with and without reporters. It is a simple but an useful study which can be considered for publication after addressing the following minor comments.

We thank the reviewer for these comments.

1. It has been well established in the literature that more than 50% of the implanted cells (either syngeneic or xenograft) tend to lose their viability within first 48 hrs and the rest over time based on the host immune system's impact on the implanted cells. BLI is a viability imaging reporter while MR contrast agent can stay in the implanted location even several days after the cells dye. In contrast BLI has poor spatial resolution and light attenuation by soft and hard tissues. Hence a combination of these two imaging reporter would be important. The authors mention these issues in their introduction and discussion section of the manuscript, but tend to ignore in their experimental approaches where no assessment for cell viability has been performed. The authors should consider evaluating at least the end point ex vivo analysis for cell viability.

We agree with the reviewer that assessing transplants longitudinally using BLI would have been ideal to assess graft viability. As discussed in the manuscript, loss of transgene expression and attenuation of the bioluminescence signal after DAPC administration meant that this was not possible. However, we have shown that transplanted human cells were alive at the experimental endpoint in all groups via immunofluorescence, using human-specific antibodies against a nuclear antigen and NCAM (see Fig. 3, Fig. 4, Fig. 5 & ESM Fig. 4). By examining the entire volume of the transplant areas, it may have been possible to quantify the total number of viable cells in each group and compare this to the number of administered cells. However, quantifying the survival ratio of transplanted cells was not the primary goal of this project; rather, we were interested in the fate of those cells that survived.

2. It is not clear how the MPIO were taken-up by the cells. It is also important to show toxicity data for these microparticles in hESC cells. Normally the SPIO and IO were transfected in cells using some transfection agents. But in this study the authors just exposed cells to MPIO without any specific agent. Hence it is important to quantify the number of particles present inside the cells.

We agree that SPIONs often require the use of transfection reagents for cellular uptake. However, as the reviewer points out, we have used magnetic particles of iron oxide (MPIOs) from Bangs Laboratories in this study. These MPIOs are coated with a polymer similar to that used in the manufacture of tissue culture vessels. This polymer matrix effectively shields the cell from the iron oxide core. As such, they do not require transfection reagents for endocytotic particle uptake and are generally non-toxic to cells. Bangs Laboratories MPIOs have been used previously to label murine pluripotent stem cell-derived neural progenitors with no observed cytotoxicity [1]. Furthermore, human mesenchymal stromal cells and foetal neural progenitors have been shown to behave normally following MPIO labelling [2]. Therefore, we do not believe that the MPIOs used in this study had any negative impact on labelled DAPCs, nor their behaviour *in vivo*. Indeed, we did not observe any qualitative difference in transplant viability when comparing MPIO-labelled DAPCs to controls (see Fig. 4e & ESM Fig. 4). Labelling efficiency was measured via flow cytometry (see Fig. 4a).

3. The quality of all the images provided in the manuscript are very poor. It is important get high contrast images for all the immunostaining results.

We thank the reviewer for bringing this to our attention. All figure panels were submitted at 300 dpi. Unfortunately, the pdf conversion system significantly reduced this resolution. We will ensure that the publisher has high-resolution figures for the accepted manuscript. Further, we have attached high-resolution versions of all figures in a compressed file for inspection following resubmission.

Reviewer #2: The submitted manuscript was very well written and the experiments were conducted and then discussed in an ideal manner including negative results (eg loss of BLI signal over time/differentiation) that would be pertinent to other researchers conducting similar research.

We thank the reviewer for these comments.

Minor comments:

1. Some fluorescent reporter genes can be partially (or fully) quenched during fixation of tissues post mortem. It may be wise to include this as a caveat when interpreting immunofluorescence histological data.

We agree that tissue fixation and subsequent processing for histological analysis can lead to partial or complete quenching of fluorescent reporters. However, this caveat is typically associated with paraffin processing (specifically the dehydration step) rather than fixation [3]. In the present study, we have cryo-embedded the post-mortem samples, which better preserves fluorescence. Furthermore, we have observed fluorescent murine mesenchymal stromal cells in frozen sections when labelled using the same Fluc-ZsGreen lentiviral reporter [4]. We also

showed that ZsGreen expression was maintained in some of the hESC-derived masses (see Fig. 2c), supporting the notion that histological processing was not the cause of fluorescence loss. Based on our experience, we believe that the loss of ZsGreen fluorescence post-mortem was due to gene silencing as DAPCs matured (as stated in the discussion), rather than as a result of histological processing. We also note that although we have imaged all tissues in the green channel in order to assess ZsGreen expression, this was not the main method we employed to identify the human cells. For that, we used immunofluorescence employing human specific antigens (human nuclei and human NCAM).

2. I am curious to why the authors chose to keep some of the individual IF microscopy channels in grey scale rather than use the colour representation as shown in the merged image. The in vitro assessments and supplementary data used colour representation in the channel images. I suggest authors display both the manuscript and supplemental images consistently and provide explanation to why using grey scale rather than colour is the optimal choice if chosen.

We chose to show individual channels in greyscale because the human perception of colour is non-linear, meaning that grayscale images are easier to see and interpret than colour images [5]. However, we thank the reviewer for pointing out inconsistencies in our presentation of main text and supplementary figures. We have now changed individual colour images to greyscale in ESM Figs. 1 & 2.

3. MPIOs can also persist in an area after uptake from bystander cells such as microglia or infiltrated peripheral macrophages. To provide further evidence that the persistent MPIOs represent persistent cells of interest the authors could stain the tissues using Perls Prussian blue to detect the nanoparticles and perform IHC for glial or macrophage markers (eg GFAP) to look for bystander cell uptake. Alternatively the cell masses could be dissected out post mortem, and assessed with flow cytometry using the fluorescence of the nanoparticles in concert with phenotyping antibodies (ie human marker vs GFAP or other glial/macrophage markers eg CD45/CD11b/CD11c etc).

Whilst Prussian blue (PB) is a useful stain for nanoparticles composed of iron, the MPIOs used in this study are surrounded by a polystyrene matrix, meaning that PB staining would only identify MPIOs bisected during sectioning. This is supported by the fact that cells labelled with MPIOs from Bangs Laboratories do not stain positive for PB in monolayer culture [6]. As such, this approach would underestimate the number of MPIOs in the transplant areas, given that the particles are approximately 1.6  $\mu\text{m}$  and cryo-sections are 7  $\mu\text{m}$ .

We agree that MPIO uptake by host immune cells is an issue of concern, which could lead to false positives. We have conducted co-staining of glial cells (GFAP) and DAPCs (hNCAM) in MPIO-labelled transplants (see Fig. 5a & ESM Fig. 4a) and we did not observe particles in glial cells. Indeed, MPIOs were localised to perinuclear regions of DAPCs and were not observed outside the transplant area.

Flow cytometric quantification of MPIO uptake by bystander immune cells could indeed provide useful information on the specific localisation of MPIOs following transplantation, but

this is beyond the scope of the current study. We will certainly consider this analysis in future projects.

## References

1. Yan YW, Sart S, Bejarano FC, et al. (2015) Cryopreservation of Embryonic Stem Cell-Derived Multicellular Neural Aggregates Labeled with Micron-Sized Particles of Iron Oxide for Magnetic Resonance Imaging. *Biotechnology Progress* 31:510-521.
2. Boulland JL, Leung DSY, Thuen M, et al. (2012) Evaluation of Intracellular Labeling With Micron-Sized Particles of Iron Oxide (MPIOs) as a General Tool for In Vitro and In Vivo Tracking of Human Stem and Progenitor Cells. *Cell Transplantation* 21:1743-1759.
3. Ouyang ZM, Zhao PL, Yang Y, Yang XQ, Gong H, Li XN (2019) Maintenance of Fluorescence During Paraffin Embedding of Fluorescent Protein-Labeled Specimens. *Frontiers in Neuroscience* 13.
4. Scarfe L, Taylor A, Sharkey J, et al. (2018) Non-invasive imaging reveals conditions that impact distribution and persistence of cells after in vivo administration. *Stem Cell Research & Therapy* 9.
5. Lee JY, Kitaoka M (2018) A beginner's guide to rigor and reproducibility in fluorescence imaging experiments. *Molecular Biology of the Cell* 29:1519-1525.
6. Taylor A, Herrmann A, Moss D, et al. (2014) Assessing the Efficacy of Nano- and Micro-Sized Magnetic Particles as Contrast Agents for MRI Cell Tracking. *Plos One* 9.



# Please wait...

If this message is not eventually replaced by the proper contents of the document, your PDF viewer may not be able to display this type of document.

You can upgrade to the latest version of Adobe Reader for Windows®, Mac, or Linux® by visiting [http://www.adobe.com/go/reader\\_download](http://www.adobe.com/go/reader_download).

For more assistance with Adobe Reader visit <http://www.adobe.com/go/acrreader>.

Windows is either a registered trademark or a trademark of Microsoft Corporation in the United States and/or other countries. Mac is a trademark of Apple Inc., registered in the United States and other countries. Linux is the registered trademark of Linus Torvalds in the U.S. and other countries.

# Please wait...

If this message is not eventually replaced by the proper contents of the document, your PDF viewer may not be able to display this type of document.

You can upgrade to the latest version of Adobe Reader for Windows®, Mac, or Linux® by visiting [http://www.adobe.com/go/reader\\_download](http://www.adobe.com/go/reader_download).

For more assistance with Adobe Reader visit <http://www.adobe.com/go/acrreader>.

Windows is either a registered trademark or a trademark of Microsoft Corporation in the United States and/or other countries. Mac is a trademark of Apple Inc., registered in the United States and other countries. Linux is the registered trademark of Linus Torvalds in the U.S. and other countries.



# Please wait...

If this message is not eventually replaced by the proper contents of the document, your PDF viewer may not be able to display this type of document.

You can upgrade to the latest version of Adobe Reader for Windows®, Mac, or Linux® by visiting [http://www.adobe.com/go/reader\\_download](http://www.adobe.com/go/reader_download).

For more assistance with Adobe Reader visit <http://www.adobe.com/go/acrreader>.

Windows is either a registered trademark or a trademark of Microsoft Corporation in the United States and/or other countries. Mac is a trademark of Apple Inc., registered in the United States and other countries. Linux is the registered trademark of Linus Torvalds in the U.S. and other countries.

# Please wait...

If this message is not eventually replaced by the proper contents of the document, your PDF viewer may not be able to display this type of document.

You can upgrade to the latest version of Adobe Reader for Windows®, Mac, or Linux® by visiting [http://www.adobe.com/go/reader\\_download](http://www.adobe.com/go/reader_download).

For more assistance with Adobe Reader visit <http://www.adobe.com/go/acrreader>.

Windows is either a registered trademark or a trademark of Microsoft Corporation in the United States and/or other countries. Mac is a trademark of Apple Inc., registered in the United States and other countries. Linux is the registered trademark of Linus Torvalds in the U.S. and other countries.



# Please wait...

If this message is not eventually replaced by the proper contents of the document, your PDF viewer may not be able to display this type of document.

You can upgrade to the latest version of Adobe Reader for Windows®, Mac, or Linux® by visiting [http://www.adobe.com/go/reader\\_download](http://www.adobe.com/go/reader_download).

For more assistance with Adobe Reader visit <http://www.adobe.com/go/acrreader>.

Windows is either a registered trademark or a trademark of Microsoft Corporation in the United States and/or other countries. Mac is a trademark of Apple Inc., registered in the United States and other countries. Linux is the registered trademark of Linus Torvalds in the U.S. and other countries.

# Please wait...

If this message is not eventually replaced by the proper contents of the document, your PDF viewer may not be able to display this type of document.

You can upgrade to the latest version of Adobe Reader for Windows®, Mac, or Linux® by visiting [http://www.adobe.com/go/reader\\_download](http://www.adobe.com/go/reader_download).

For more assistance with Adobe Reader visit <http://www.adobe.com/go/acrreader>.

Windows is either a registered trademark or a trademark of Microsoft Corporation in the United States and/or other countries. Mac is a trademark of Apple Inc., registered in the United States and other countries. Linux is the registered trademark of Linus Torvalds in the U.S. and other countries.

# Please wait...

If this message is not eventually replaced by the proper contents of the document, your PDF viewer may not be able to display this type of document.

You can upgrade to the latest version of Adobe Reader for Windows®, Mac, or Linux® by visiting [http://www.adobe.com/go/reader\\_download](http://www.adobe.com/go/reader_download).

For more assistance with Adobe Reader visit <http://www.adobe.com/go/acrreader>.

Windows is either a registered trademark or a trademark of Microsoft Corporation in the United States and/or other countries. Mac is a trademark of Apple Inc., registered in the United States and other countries. Linux is the registered trademark of Linus Torvalds in the U.S. and other countries.

# Please wait...

If this message is not eventually replaced by the proper contents of the document, your PDF viewer may not be able to display this type of document.

You can upgrade to the latest version of Adobe Reader for Windows®, Mac, or Linux® by visiting [http://www.adobe.com/go/reader\\_download](http://www.adobe.com/go/reader_download).

For more assistance with Adobe Reader visit <http://www.adobe.com/go/acrreader>.

Windows is either a registered trademark or a trademark of Microsoft Corporation in the United States and/or other countries. Mac is a trademark of Apple Inc., registered in the United States and other countries. Linux is the registered trademark of Linus Torvalds in the U.S. and other countries.



# Please wait...

If this message is not eventually replaced by the proper contents of the document, your PDF viewer may not be able to display this type of document.

You can upgrade to the latest version of Adobe Reader for Windows®, Mac, or Linux® by visiting [http://www.adobe.com/go/reader\\_download](http://www.adobe.com/go/reader_download).

For more assistance with Adobe Reader visit <http://www.adobe.com/go/acrreader>.

Windows is either a registered trademark or a trademark of Microsoft Corporation in the United States and/or other countries. Mac is a trademark of Apple Inc., registered in the United States and other countries. Linux is the registered trademark of Linus Torvalds in the U.S. and other countries.



# Please wait...

If this message is not eventually replaced by the proper contents of the document, your PDF viewer may not be able to display this type of document.

You can upgrade to the latest version of Adobe Reader for Windows®, Mac, or Linux® by visiting [http://www.adobe.com/go/reader\\_download](http://www.adobe.com/go/reader_download).

For more assistance with Adobe Reader visit <http://www.adobe.com/go/acrreader>.

Windows is either a registered trademark or a trademark of Microsoft Corporation in the United States and/or other countries. Mac is a trademark of Apple Inc., registered in the United States and other countries. Linux is the registered trademark of Linus Torvalds in the U.S. and other countries.

# Please wait...

If this message is not eventually replaced by the proper contents of the document, your PDF viewer may not be able to display this type of document.

You can upgrade to the latest version of Adobe Reader for Windows®, Mac, or Linux® by visiting [http://www.adobe.com/go/reader\\_download](http://www.adobe.com/go/reader_download).

For more assistance with Adobe Reader visit <http://www.adobe.com/go/acrreader>.

Windows is either a registered trademark or a trademark of Microsoft Corporation in the United States and/or other countries. Mac is a trademark of Apple Inc., registered in the United States and other countries. Linux is the registered trademark of Linus Torvalds in the U.S. and other countries.